[7]B. Basu *et al.*, in *Proceedings of the Sixth International Conference on Plasma Physics and Controlled Nuclear Fusion Research, Berchtesgaden, West Germany, 1976* (International Atomic Energy Agency, Vienna, 1977), Vol. 2, p. 455.
[8]K. Molvig, Bull. Am. Phys. Soc. 21, 1125 (1976).
[9]M. H. Hughes *et al.*, to be published.
[10]J. E. Rice and H. I. Helava, Bull. Am. Phys. Soc. 21, 1141 (1976).
[11]J. L. Terry *et al.*, John Hopkins University, Technical Report No. COO-2711-3, 1977 (unpublished).
[12]A. Gondhalekar, D. Overskei, R. R. Parker, and J. West, to be published.
[13]M. H. Hughes and D. E. Post, Princeton Plasma Physics Laboratory Report No. 1335, 1977 (to be published).

Observation of Severe Heat-Flux Limitation and Ion-Acoustic Turbulence in a Laser-Heated Plasma

D. R. Gray, J. D. Kilkenny, and M. S. White
Blackett Laboratory, Imperial College, London, United Kingdom

and

P. Blyth and D. Hull
Atomic Weapons Research Establishment, Aldermaston, United Kingdom

(Received 12 September 1977)

The thermal conductivity of a plasma of density 6×10^{16} cm^{-3} is measured when it is heated by a 300-MW, 3-ns CO_2 laser pulse. The data are best represented using a heat flux which is limited to $\sim 4\%$ of the free-streaming limit. Low-frequency turbulence is observed of sufficient intensity to cause this flux limit.

In this Letter we report definitive measurements of the thermal conductivity of a laser-heated plasma when the temperature gradient is large and an ion-acoustic instability is excited. The classical treatment of thermal conductivity[1] has been by a first-order perturbation to a Maxwellian. However, when λ_e/L (the ratio of the electron mean free path to the temperature-gradient scale length) is greater than 0.02, second-order terms dominate and there seems to be no rigorous theory. Here we use

$$\lambda_e/L = 2.292\times10^{13}T_e\,|\nabla T_e|\,n_e\ln\Lambda, \qquad (1)$$

with T_e in eV and n_e in inverse cubic centimeters. We have previously measured the thermal conductivity[2] with $T_e = T_i$ and $\lambda_e/L \sim 0.04$ and found a reduction by a factor of 2 from Spitzer's value. When $T_e \gg T_i$, the return current from the heat flow can drive an ion-acoustic instability, which would decrease the heat flux.[3,4] Here we have increased λ_e/L to 0.5 (from Ref. 2) and with $T_e \sim 5T_i$ have seen a very low thermal conductivity accompanied by low-frequency turbulence.

As before, our measurement is based on ruby-laser light scattering. We have extended this technique to spatial and temporal resolutions of 200 μm and 1 ns. Other experiments on laser-produced plasmas[5-7] have used much less direct diagnostics to measure thermal conductivity. Many other phenomena (magnetic-field generation, resonant absorption, atomic physics, fast-electron transport) complicate these experiments. In contrast, our experiment has to our knowledge none of these extraneous phenomena.

The plasma used has been described previously.[2] It was a weak hydrogen Z pinch with initial density and temperature of 6×10^{16} cm^{-3} and 4 eV, respectively. The center of this plasma was heated by a 300-MW, 3-ns CO_2 laser pulse, focused to a measured spot size of 350 ± 50 μm. Ruby-laser light scattering at 90° was performed with the differential scattering vector ($\vec{k}_s$) both parallel and perpendicular to ∇T_e. The scattering parameter α was in the range $0.5<\alpha<1.5$. The electron density and temperature were obtained by fitting shifted Salpeter curves for different α's to the electron features. This method is described by Kunze.[8] The error bars on density and temperatrue were determined by the range of the values of α which would fit within the experimental error bars. These values of n_e agreed with those obtained using a Rayleigh calibration of the system. A fast photomultiplier (RCA C31024A) gave a 1.2-ns time resolution. Reproducibility was good enough to plot spectra on a shot-to-shot basis. The spatial resolution

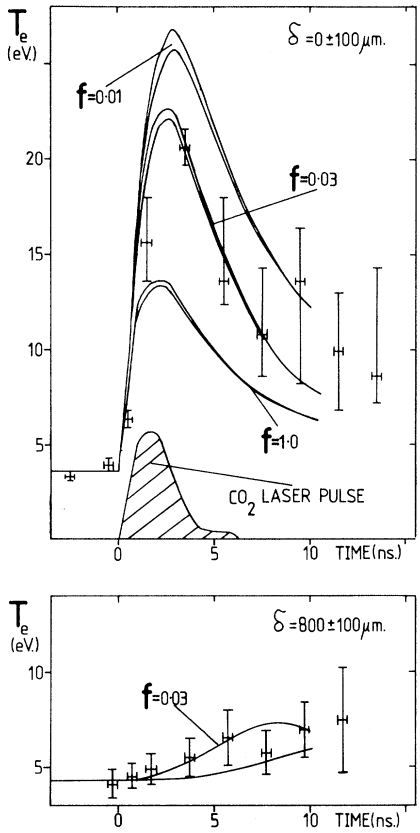

FIG. 1. Examples of experimental data and simulation results with $s = 1$ and $w = 1$. For each simulation the two solid lines indicate the band of temperature possible within the ± 100-μm alignment setting error. At $\delta = 0$, the best fit of $f = 0.03$ is shown together with $f = 1.0$ and $f = 0.01$. At $\delta = 800$ μm the band is for displacements between 700 and 900 μm and simulation results are only shown for $f = 0.03$.

(~200 μm) was defined by the spectrometer entrance-slit height and width, and the measured ruby-laser focal-spot size. Data were taken for different displacements (δ) between the CO_2- and ruby-laser foci.

On the length and time scale of the laser heating, the plasma was homogeneous, constant, and unmagnetized. As the plasma was so underdense, refraction and variation along the laser beam were negligible, and the experiment could be modeled by a one-dimensional, two-temperature fluid code with symmetry about the CO_2 laser axis.

In the simulation, the absorption coefficient K_I for CO_2 laser radiation was taken from Billman and Stallcop[9]:

$$K_I = w C_2 \lambda^2 n_e{}^2 T_e{}^{-1.5}(1 - C_3 n_e \lambda^2)^{-0.5} g, \qquad (2)$$

where w was an additional factor allowing for artificial variation of K_I. The ponderomotive force and the saturation of inverse bremsstrahlung were included although their effect was small. The electron heat flux q was defined in the normal way:

$$\vec{q} = -s\sigma T_e{}^{2.5} \nabla T_e / \ln\Lambda, \qquad (3)$$

where s is a factor allowing for an artificial variation in the conductivity. When $s = 1$ the conductivity corresponds to Spitzer's value.[1] Additionally, simulations were run in which $\vec{q}$, as defined by Eq. (3), was constrained not to exceed some fraction (f) of the free-streaming limit, $q_{max} = nkT_e(2kT_e/\pi m_e)^{0.5}$. Experiments were performed with CO_2-laser-pulse durations of 3 and 20 ns. An example of the results for $\delta = 0 \pm 100$ and $\delta = 800 \pm 100$ μm is shown in Fig. 1. Results were also obtained at $\delta = 100 \pm 100$ and 1200 ± 100 μm. On the rising edge of the heating there are large error bars due to the 1-ns instrumental time resolution. Late in time the power of the diagnostic laser is decreasing and the error bars again become large. Simulation results with $w = 1$ (classical absorption) and varying f are also shown on Fig. 1. A good fit at both displacements, where the band of simulation results fits within all the experimental errors, is obtained for $f = 0.03$, but not for $f = 1$ or $f = 0.01$. Under no conditions can $f = 1$ fit the experimental data. If, for example, the absorption coefficient is doubled for $f = 1$ the temperature at $\delta = 0$, $t = 3.5$ ns is only 14 eV compared with a measured 20.6 ± 1 eV (Fig. 1, top), and at $\delta = 800 \pm 100$ μm, $t = 3.7$ ns it is 8 ± 1 eV compared with 5.5 ± 1 eV (Fig. 1, bottom). Thus by requiring the simulations to fit the experiment at all four positions, and also for runs with the two different pulse lengths, both absorption and thermal conductivity were determined. The accuracy of the measurements of thermal conductivity and absorption is shown in Fig. 2. The hatched area shows the only regions of absorption/conductivity space where the simulation fits all the data.

Computations were also carried out in $(s, w, f = 1)$ space but the fits to the experimental data were poor. (The nearest fit was actually with $s = 0.065$, $w = 1.4$, and $f = 1$). So the comparison of experimental and simulation results for the high-intensity experiment unambiguously show best agreement for classical inverse bremsstrahlung absorption with thermal conduction modeled classically up to a (2–5)% flux limiter.

In constrast, the lower-power experiment[2] gave

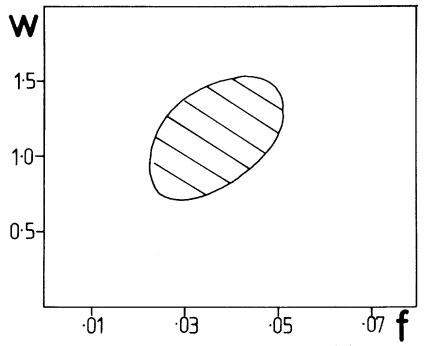

FIG. 2. Hatched area shows region of $(f, w, s = 1)$ space allowed by results. The factors w and f vary the absorption and flux limit, respectively.

good agreement between experiment and simulation for classical absorption and a heat flux of 0.4 times Spitzer's value without using a flux limiter ($s = 0.4$, $w = 1$, and $f \geq 0.05$). Attempts to use a model with classical ($s = 1$) thermal conduction and a flux limiter gave much poorer fits, the least bad being with $s = 1$, $w = 1$, and $f = 0.06$.

The measured n_e and T_e defined a thermal level $S_{i,\mathrm{th}}$ for scattering in the ion feature.[8] At $\delta = 0$, where the scattered electron spectra were symmetric and thermal, the height of the observed ion feature (S_{i0}) is enhanced to $\sim 14 S_{i,\mathrm{th}}$ as shown in Fig. 3. S_{i0} was obtained from the measured scattering in a 13-Å-bandwidth channel centered at the ruby wavelength, after the small stray-light and the electron-feature contributions had been subtracted.

The results of the two experiments are summarized and compared with Spitzer's theory in Fig. 4. In the low-power experiment,[2] matching of experimental and computational results showed that, for temperature gradients characterized by $\lambda_e/L \lesssim 0.04$, the heat flux was best modeled by reducing the classical thermal conduction coefficient to 0.4 ± 0.2 times Spitzer's value. The discrepancy is attributed to the failure of Spitzer's first-order perturbation theory for $\lambda_e/L \gtrsim 0.02$. The simulation could not be made to fit the experiment well for reduced thermal conduction based on a flux limiter. No evidence of ion-acoustic turbulence was observed or expected since the long (70-ns) CO_2-laser pulse allowed equilibration of T_e and T_i to within about 10%.

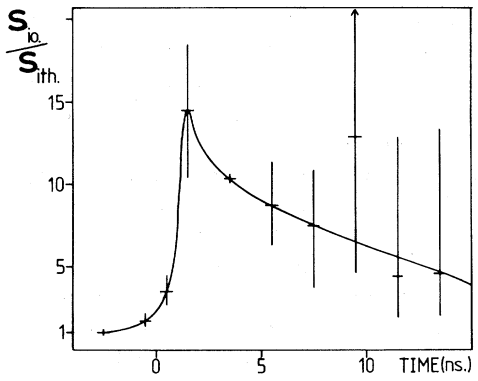

FIG. 3. Enhancement above thermal of scattering in the ion feature. The 3-ns CO_2-laser pulse starts at time zero.

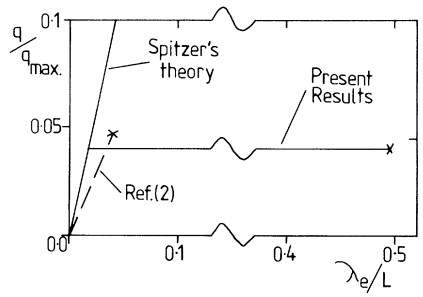

FIG. 4. Normalized heat flux vs normalized temperature gradient showing strong heat-flux limitation.

In the high-power experiment the temperature gradient λ_e/L was increased from 0.04 to 0.5 but the normalized heat flux $q/q_{\max}$ was no higher than in the low-power case. The experiment was best modeled by the simulation using classical thermal conduction up to $\lambda_e/L \simeq 0.02$, then a flux limiter of 0.02 to 0.05 times the free-streaming limit. Although a theory for large temperature gradients does not exist, it would be reasonable to expect that in the absence of turbulence $q/q_{\max}$ would increase as λ_e/L increases. The fact that it did not we attribute to ion-acoustic turbulence because we observe an enhanced ion feature (Fig. 3).

Unfortunately, this observation was with $k_s \sim 2/\lambda_D$ (as $\alpha \sim \frac{1}{2}$). From simulations of current-driven ion-acoustic turbulence,[10] the spectral function $S(k)$ peaks at $1/\lambda_D$ and is much smaller at $2/\lambda_D$. Using our measurement at $2/\lambda_D$ and the shape of $S(k)$ from simulations, a fluctuation level $\delta n/n$ of 9% was deduced. From Ref. 4 this would severely limit the heat flux. It is interesting that although ion-acoustic turbulence reduces the thermal conductivity it does not increase the absorption. This is in agreement with theory[11] and is because the density is so much below critical.

The turbulence is presumed to be driven by the return current. We rule out Brillouin backscatter as the source of the turbulence because no back-

scattered light was observed at these densities and the enhancement (Fig. 3) lasted for longer than the CO_2-laser pulse (Fig. 1). The threshold for the heat-flux instability is $\lambda_e/L = 0.6$ for $T_e = 5T_i$[3], which is close to our observed maximum, $\lambda_e/L \sim 0.5$. However the distribution functions[1] on which this theory is based are unphysical since they become negative on one side in the region of velocity space where the net heat flux occurs ($1.5v_{th} < v < 3v_{th}$) when $\lambda_e/L > 0.02$.

In conclusion we have observed a (2–5)% flux limit to heat flow when $T_e \sim 5T_i$, which can be explained by the observed low-frequency turbulence.

This work was supported by the Science Research Council and the Northern Ireland Department of Education.

[a]Present address: Rutherford Laboratory, Chilton, Didcot, Oxon, United Kingdom.

[1]L. Spitzer, *Physics of Fully Ionized Gases* (Wiley, London, 1962).
[2]M. S. White, J. D. Kilkenny, and A. E. Dangor, Phys. Rev. Lett. 35, 524 (1975).
[3]D. W. Forslund, J. Geophys. Res. 75, 17 (1970).
[4]W. M. Manheimer, Phys. Fluids 20, 265 (1977).
[5]P. M. Campbell *et al.*, Phys. Rev. Lett. 39, 274 (1977).
[6]R. C. Malone, R. L. McCrory, and R. L. Morse, Phys. Rev. Lett. 34, 721 (1975).
[7]B. Yaakobi and T. C. Bristow, Phys. Rev. Lett. 38, 350 (1977).
[8]H. J. Kunze, in *Plasma Diagnostics*, edited by W. Lochte-Holtgreven (North-Holland, Amsterdam, 1968), p. 594.
[9]K. W. Billman and J. R. Stallcop, Appl. Phys. Lett. 28, 704 (1976).
[10]C. Dum, R. Chodura, and D. Biskamp, Phys. Rev. Lett. 32, 1231 (1974).
[11]R. J. Faehl and W. L. Kruer, Phys. Fluids 20, 55 (1977).

Kinetic Description of Ponderomotive Effects in a Plasma

R. E. Aamodt
Science Applications, Inc., Boulder, Colorado 80302

and

M. C. Vella
United Technologies Research Center, East Hartford, Connecticut 06108

(Received 23 May 1977)

The kinetic treatment of the ponderomotive force concept is found from nonresonant quasilinear theory for waves with spatially dependent amplitude. In general, the ponderomotive effect appears as a velocity-space diffusion term, not just as a force. For an unmagnetized plasma, the qualilinear equations are solved directly, and the correct density modification exhibited explicitly. Examples are considered for both a homogeneous and an inhomogeneous magnetic field, and aspects of rf end plugging are discussed.

The effects of electromagnetic waves on a plasma are relevant to problems in both laser fusion and magnetic confinement. In the former case, self-focusing density modifications, parametric instabilities, and magnetic field generation are of interest, and, in the latter, wave heating, end plugging of open systems, and impurity control. For many of these problems, the collisionless regime is appropriate, and both single-particle and fluid treatments have shown that the ponderomotive force plays a key role in nonresonant nonlinear phenomena. In this Letter, the inadequacy of using only a ponderomotive force in a kinetic treatment is demonstrated, and the porper collisionless kinetic theory of nonresonant wave effects in a weakly inhomogeneous plasma is presented.

When fluctuating wave amplitudes are small and autocorrelation times are short compared with diffusion times, the lowest-order wave modifications of the particle distribution are given by quasilinear theory. In this approximation, it is known that nonresonant particles acquire an apparent temperature due to the nonlinear interaction with the waves.[1] This "fake diffusion" has been used in calculating saturation amplitudes of unstable waves,[1,2] and is reconsidered here in order to understand ponderomotive effects in a weakly inhomogeneous plasma.

In one dimension, consider an electrostatic